SHOT NOISE THERMOMETRY WITH CARBON NANOTUBES

Robert A. Sayer and Timothy S. Fisher
Department of Mechanical Engineering and
Birck Nanotechnology Center
Purdue University
West Lafayette, IN 47907-2057, USA
Phone: (765) 494-5627
Fax: (765) 494-0539
E-mail: tsfisher@purdue.edu

ABSTRACT

A carbon nanotube (CNT) thermometer is reported that operates on the principles of electrical shot noise. Shot noise thermometry is a self calibrating measurement technique that relates statistical fluctuations in dc current across a device to temperature. A self-heating shot noise model has been developed and applied to experimental data to determine the thermal resistance of a CNT device consisting of an array of vertical CNTs supported in a porous anodic alumina template. The thermal resistance is found to be $1.5*10^8$ K/W.

KEY WORDS carbon nanotubes, electrical noise, shot noise, thermal resistance, thermometry

NOMENCLATURE

e	electron charge
f	frequency
h	Planck's constant
I	current
k_B	Boltzmann's constant
Q	heat rate
R	electrical resistance
R_θ	thermal resistance
S_I	current spectral density
S_V	voltage spectral density
T	device temperature
T_∞	ambient temperature
V	voltage
W	average energy associated with each oscillating mode

Subscripts

J	Johnson
s	shot

INTRODUCTION

Continued reductions in the size of engineered micro- and nano-scale devices have created a critical need for improved thermal transducers to characterize effects such as heat conduction mechanisms, electrical self-heating, and phase change phenomena at ultra-small scales. An ideal transducer would be spatially compact, be self-calibrating and allow non-invasive *in situ* measurements. Further, because of their ultra-small sizes, such transducers could be designed in integrated platforms that would bring unprecedented spatial, temporal, and statistical resolution.

Today, most solid-state thermometers for small-scale measurements employ a technique that relates changes in electrical resistance to temperature. Devices used in such resistance thermometry must have a resistance-temperature curve that is calibrated with high accuracy and precision. Also, the device's resistance must remain stable over time to prevent measurement drift and frequent recalibration. For nanoscale objects, particularly nanowires and nanotubes, satisfying these conditions is particularly challenging. For example, small changes in synthesis conditions can lead to large changes in the resistivity of multi-walled carbon nanotubes (MWCNTs)[1]. Further, the resistance of single-walled carbon nanotube (SWCNT) devices has been shown to vary dramatically with contact type, channel length, and conducting type [2-5] and such variability greatly limits the applicability of resistance thermometry in these devices. In addition, the small temperature coefficient of resistance of CNTs (typically 1-2 orders of magnitude lower than typical metals used in resistance thermometry such as Pt [6]) reduces transducer resolution. Furthermore, other researchers have found that CNTs have a negative temperature coefficient of resistance [7-9], which requires modification of typical resistance thermometry.

An alternative approach to temperature measurements in CNTs involves the fabrication of a structure that resembles a common mercury thermometer. The first such thermometer was reported by Gao and Bando in 2002 [10] and involved filling the hollow CNT core with gallium. Although an intriguing development, widespread application of this type of CNT thermometer is limited owing to the fact that the Ga level must be monitored by an electron microscope. Liu *et al.* [11] simplified the previous technique by eliminating the initial calibration step and decreased the error of measurement below 5%. Dorozhkin *et al.* [12] utilized a two order of magnitude difference in the resistivity of a Ga filled portion of a CNT compared to an empty CNT to relate the electrical resistance of a Ga-filled CNT to its temperature. This method allows real-time measurement of temperature changes. However, calibration of the thermometer is very complicated and time-consuming, and the temperature-

978-1-4244-1701-8/08/$25.00 ©2008 IEEE

dependent electrical resistivity of the Ga filled CNT and empty CNT must be measured using an atomic force microscope (AFM).

Although the foregoing developments in nanoscale thermometers are highly innovative, all such thermometers require calibration that can be complicated and sample-specific. Noise thermometry offers a compelling alternative to resistance thermometry for nanoscale objects. A shot noise thermometer made from a CNT would act as a self-calibrating transducer that accommodates variations in electrical behavior that are difficult and sometimes impossible to control precisely.

Sensors used to measure temperature can be divided into two groups: primary and secondary thermometers. Primary thermometers are characterized by well established state equations that relate the measured quantity to temperature through a simple physical principle. These thermometers are capable of providing absolute temperature without calibration, while secondary thermometers such as those that exploit changes in electrical resistance must be calibrated to a known temperature. Most primary thermometers are expensive and difficult to operate. However, electrical noise measurements can provide a simple basis for creating primary thermometers that are capable of accurate temperature measurements in the range from a 1 mK to greater than 1500 K [13] This paper presents results from a carbon nanotube sensor that utilizes a unique combination of innovative nanofabrication processes and a primary temperature measurement approach that exploits nanoscale transport principles.

THEORY

Johnson Noise

The valence electrons in electrical conductors are free to move as a so-called electron gas. Even in the absence of an applied bias, statistical fluctuations of the electric charge in the conductor occur due to the random movement, or Brownian motion, of the electrons caused by thermal agitation. This effect was first observed and measured for various conductors using a vacuum tube amplifier by Johnson [14, 15] and was explained theoretically by his colleague, Nyquist [16], using the equipartition theorem. This effect of thermal noise garners its name from the early pioneers of the field as Johnson-Nyquist or simply Johnson noise.

From quantum theory, the average energy W associated with each oscillating mode of frequency f is given by

$$W = \frac{hf}{\exp\left(\frac{hf}{k_B T}\right) - 1} \tag{1}$$

where h is Planck's constant, k_B is the Boltzmann constant, and T is temperature. If $hf \ll k_B T$, Eq. (1) reduces to $W \approx k_B T$. The voltage spectral density S_V and current spectral density S_I are expressed as

$$\begin{aligned} S_{V,J} &= 4k_B TR \\ S_{I,J} &= \frac{4k_B T}{R} \end{aligned} \tag{2}$$

where R is the resistance of the conductor which may vary with frequency and the subscript J denotes Johnson noise. Equation (2) is independent of frequency and is valid for frequencies up to several GHz at room temperature [17].

Shot Noise

Shot noise, first reported by Schottky [18], occurs in any system in which discrete charge carriers tunnel from a cathode to an anode, such as in cold cathodes and tunnel junctions. Electron transport through a tunnel junction is statistical in nature and depends on the size of the barrier as well as the potential between the anode and cathode. Although the current averaged over a sufficiently long time through the junction is constant in time under a steady applied bias, the rate of electrons passing through the junction fluctuates randomly at short time scales. Each electron that tunnels through a barrier can be considered as a discrete 'shot' or impulse of charge and can be represented by a Dirac delta function. The current spectral density of shot noise is [19]

$$S_{I,s} = 2eI \tag{3}$$

where e is the electron charge, I is the average current, and the subscript s denotes shot noise. Like Johnson noise, shot noise is independent of frequency up to several GHz.

Because shot noise is independent of temperature, it may appear to be of little use in temperature measurements. However, when measured in combination with Johnson noise, Spietz *et al.* [20, 21] showed recently that shot noise can be exploited to achieve accurate temperature measurements from the mK range to hundreds of Kelvin. The current spectral density for combined Johnson and shot noise is given as

$$S_{I,J+s} = 2eI \coth\left(\frac{eV}{2k_B T}\right) \tag{4}$$

At zero applied bias this equation reduces to the Johnson form, $S_{I,s} = 4k_B T/R$; and at large applied biases it approaches the shot noise limit, $S_{I,s} = 2eI$.

ANALYSIS

Self-Heating Model

The prior discussion assumes that temperature of the device under test remains constant with applied voltage. In practice, the temperature of the device varies with bias due to joule heating. Accounting for self-heating, Eq. (4) can be written

$$S_{I,J+s} = 2eI \coth\left(\frac{eV}{2k_B T(V)}\right) \quad (5)$$

where the voltage-dependent temperature is given by

$$T(V) = QR_\theta + T_\infty \quad (6)$$

and where $Q = V^2/R$ is the heat rate, T_∞ is the ambient temperature, R and R_θ are the electrical and thermal resistance, respectively. In SWCNTs, significant self-heating occurs when the power density is greater than 5 μW/μm [22]. Substituting Eq. (6) into Eq. (5), the temperature-dependent shot noise relation is

$$S_{I,J+s} = 2eI \coth\left(\frac{eV}{2k_B (QR_\theta + T_\infty)}\right) \quad (7)$$

The thermal resistance of a CNT device will be dominated by the nanotube-substrate interface [23]. The minimum thermal resistance for an individual single-walled carbon nanotube at cryogenic conditions will be bounded by the quantum of thermal resistance [24, 25]. Shi *et al.* [26] measured the thermal resistance of suspended SWCNT bundles using a microfabricated device to be ≈4*10^8 K/W and ≈5*10^7 K/W for bundles of diameter 10 nm and 148 nm, respectively. Dames *et al.* [27] used a hot wire technique to measure the thermal resistance of individual MWCNTs contacted with liquid Ga inside a transmission electron microscope. They report a value of 3.3*10^7 K/W for the combined thermal resistance of the CNT and contacts.

EXPERIMENTAL SETUP

Device Fabrication

The CNT thermometer is composed of vertical SWCNT elements fabricated in a porous anodic alumina (PAA) template with an embedded Fe catalyst layer (Fig. 1a) according to a process recently reported [5, 28-30]. Carbon nanotubes were grown in the PAA template with a microwave plasma chemical vapor deposition (MPCVD) system. The CNT synthesis was conducted at a substrate temperature of 900°C with gas flow rates of 50 sccm H_2 and 10 sccm CH_4 and a plasma power of 300 W.

Subsequently, Pd nanowires were electrodeposited into the pore bottoms (Fig. 1b) to make an electrical contact to the CNTs [28]. 50 x 50 μm^2 top contacts (Fig. 1c) of Pd/Ti/Au were defined using photolithography and deposited via electron beam evaporation. The final device was inspected with a cold field emission scanning electron microscope (FESEM) (Hitachi S-4800). A tilted view of the top contact is shown in Fig. 1d. The image of the top contact on that was evaporated onto the CNT covered PAA surface. The CNTs can be appear as bright lines on the top alumina surface due to electron beam charging effects [29]. The inset shows a cross sectional view prepared by fracture of the structure.

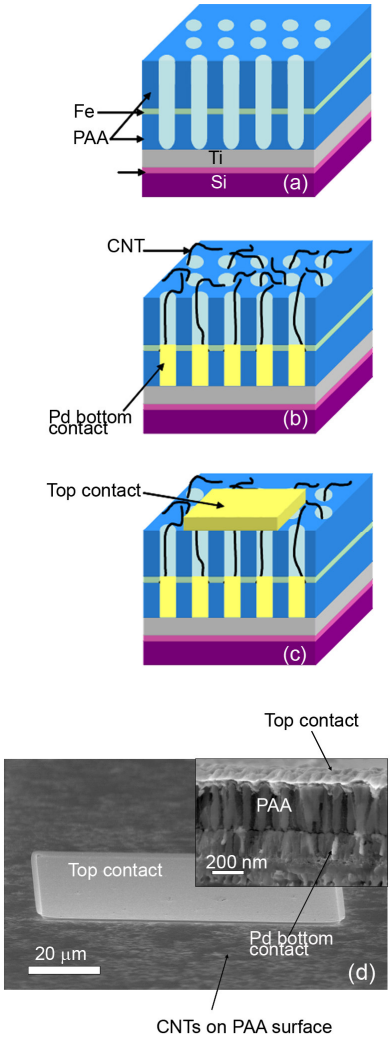

Fig. 1: Fabrication procedure for the CNT shot noise thermometer. (a) PAA with an embedded Fe layer is used as a template. (b) SWCNTs are grown at a density of one per pore and Pd nanowires are deposited. (c) A top contact is evaporated to the CNT tips. (d) Tilted FESEM image of the final device. The 50 x 50 μm^2 top contact pad is shown on top of the CNT covered PAA surface. CNTs appear as bright lines covering the PAA surface. (inset) Cross-sectional view .of the final device (Courtesy A. Franklin).

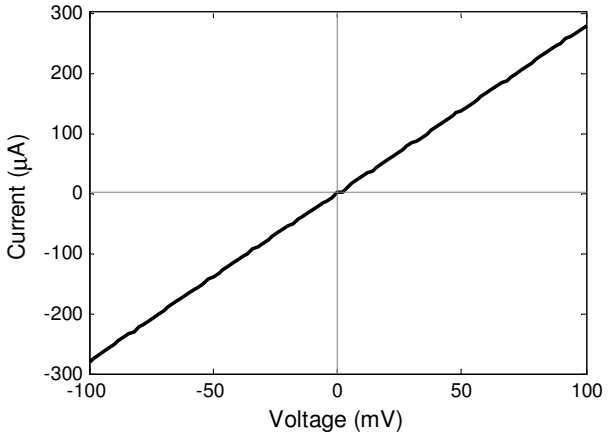

Fig. 2: Room temperature *I-V* characteristics of a typical vertical SWCNT device.

Room temperature *I-V* characteristics of the device are shown in Fig. 2. The linear relationship between voltage and current signifies ohmic contacts. The overall device resistance was 359 Ω. Maschmann *et al.* [5] measured the resistance of an individual SWCNT in a PAA template using a conductive atomic force microscope (CAFM) to be ~200 kΩ for an estimated CNT length of approximately 10 μm. The device reported here has a channel length of 400 nm: therefore 200 kΩ is taken as an upper bound of the resistance of an individual CNT. de Pablo *et al.* [31] found that the resistance of SWCNTs scales exponentially with channel length and measured the minimum resistance of a 400 nm long SWCNT dispersed on a SiO_2 substrate to be approximately 70 kΩ. This value is used as a lower bound. Assuming that all of the CNTs in the test device are connected electrically in parallel, we estimate the number of contacted tubes to be in the range of 200-600.

Measurement System

A constant dc voltage is applied across a SWCNT device that is placed inside a shielded probe station in order to minimize external noise sources. The noise across the device is then amplified with a low noise current preamplifier (LNA) (Stanford Research Systems SR570) and measured with a spectrum analyzer (Agilent 35670A) as shown in Fig. 3.

RESULTS

Direct current voltage biases ranging from 0 to 80 mV were applied to the CNT array in a room temperature (296 K) ambient within a shielded probe station. The current spectral density from 3-100 kHz was measured. 150 RMS data averages were computed to minimize statistical fluctuations in the measured noise spectra. The current spectral density of noise is shown in Fig. 4 for several different voltages. Instrument noise (resulting from both the spectrum analyzer and LNA) was measured and found to be constant with dc bias. This value of this instrument noise floor was subtracted from the subsequent measurements.

At frequencies below 60 kHz, the spectra are dominated by 1/*f* noise, consistent with previous studies [32-34]. Also, the slight divergence of the noise levels approaching the highest frequency (10^5 Hz) is a result of reaching the frequency limit of the spectrum analyzer. At intermediate frequencies, the

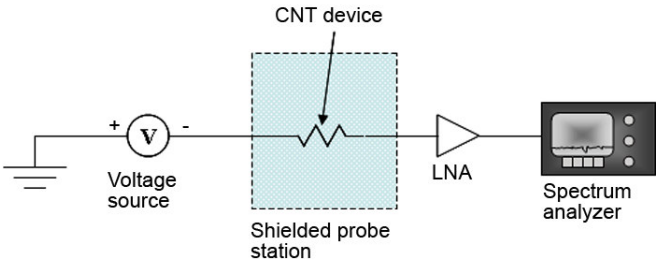

Fig. 3: Schematic of the setup used to measure electrical noise. The spectrum analyzer (Agilent 35670A) is rated for measurements from dc to 102.4 kHz and the LNA had a gain 200 μA/V.

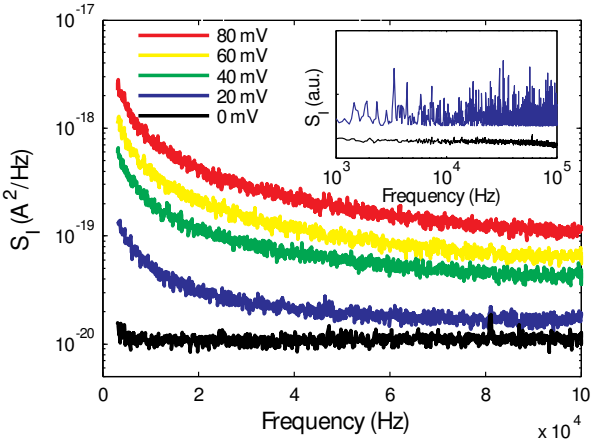

Fig. 4: Current spectral density measured across the CNT device. 1/*f* noise dominates the signal at frequencies below 60 kHz. Shot noise is observed at frequencies above 60 kHz. (inset) Measured current spectral density at 0 mV using (blue) 1 and (black) 200 RMS data averages.

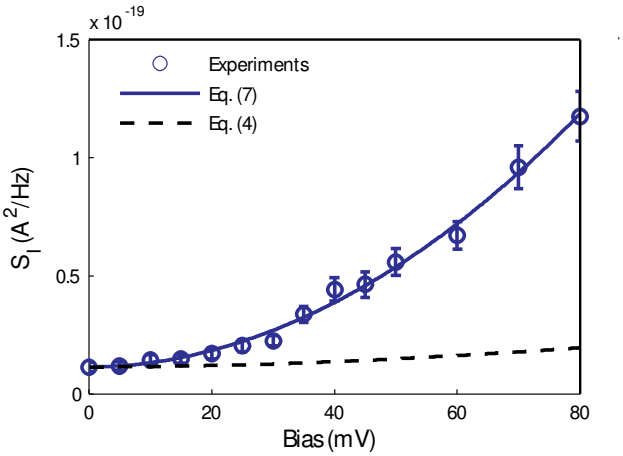

Fig. 5: Experimentally measured shot noise current spectral density as a function of dc bias voltage. The dashed line is the value predicted with out self-heating and the solid line is a fit to the data including self-heating. $R_\theta = 2.7*10^7$ K/W. The error bars represent one standard deviation from the mean upon averaging over the frequency independent portion of the spectrum.

measured noise is independent of frequency, but its average magnitude varies with applied dc bias as is characteristic of shot noise. The inset of Fig. 4 shows the measured noise signal at 0 mV with 1 and 150 averages. The curves are offset vertically to enable visual distinction between the two. Although both measurements fluctuate about the same mean value, averaging reduces the amplitude of these fluctuations.

The average current spectral density (averaged over the frequency independent portion of the spectrum) is shown in Fig. 5 for dc biases ranging from 0-80 mV. The error bars in the figure represent one standard deviation from the mean value averaged over the range 79 to 100 kHz. Notably, the self-heating model (Eq. 7) accurately predicts the shape of the measured shot noise curve, whereas an isothermal model

(Eq. 4) fails to capture the trend in noise with increasing voltage bias. A fit of the average noise data to Eq. (7) yields a thermal resistance of $1.5*10^8 \pm 0.1*10^8$ K/W, where the uncertainty is based on the 95% confidence interval of the curve fit. The order of magnitude of the resulting thermal conductance per unit CNT length (with a 100nm array height) is therefore $g \sim 0.1$ W/Km . Notably, this results agrees well with a recent estimate by Pop *et al.* [22] of overall thermal conductance for a self-heated metallic SWCNT on a dielectric substrate based on a combination of experimental measurements and coupled electro-thermal transport models.

The temperature rise in the CNT device can be calculated from Eq. (6). At the highest biases measured, the temperature rise is on the order of 10^3 K. While this projection seems unexpectedly high, we note that current will almost certainly channel through the least resistive pathways in the massively parallel array, and therefore, heat dissipation is expected to be localized to a small fraction of the total number of CNTs. Temperature rises of this magnitude have been previously observed in individual SWCNTs suspended in a vacuum [35, 36]. Further work is ongoing to isolate such effects by studying individual CNT devices and small areas of the structure discussed above.

CONCLUSION

Shot noise of a device consisting of a parallel array of vertical CNTs supported in a PAA substrate has been measured. The magnitude of the shot noise does not follow the expected curve for an isothermal device. Rather, a substantial deviation due to significant self-heating of the CNT device is observed. A simple self-heating shot noise model that assumes constant device resistance has been developed and fit to the measured data. The resulting thermal resistance of the CNT device is found to be $1.5*10^8 \pm 0.1*10^8$ K/W.

ACKNOWLEDGMENTS The authors would like to thank Sunkook Kim for his assistance with setting up the noise measurements and Aaron Franklin for contributing to the development of the CNT-PAA devices.

REFERENCES

[1] C. Lan, et al., "Correlating electrical resistance to growth conditions for multiwalled carbon nanotubes," *Applied Physics Letters*, vol. 91, no. 9, 2007, pp. 093105.
[2] A. Javey, et al., "Ballistic carbon nanotube field-effect transistors," *Nature*, vol. 424, no. 6949, 2003, pp. 654-657.
[3] Y. Li, et al., "Preferential Growth of Semiconducting Single-Walled Carbon Nanotubes by a Plasma Enhanced CVD Method," *Nano Lett.*, vol. 4, no. 2, 2004, pp. 317-321.
[4] J.Y. Park, et al., "Electron-Phonon Scattering in Metallic Single-Walled Carbon Nanotubes," *Nano Lett.*, vol. 4, no. 3, 2004, pp. 517-520.
[5] M.R. Maschmann, et al., "Lithography-Free in Situ Pd Contacts to Templated Single-Walled Carbon Nanotubes," *Nano Lett.*, vol. 6, no. 12, 2006, pp. 2712-2717.
[6] K. Liu, et al., "Electrical transport in doped multiwalled carbon nanotubes," *Physical Review B*, vol. 63, no. 16, 2001, pp. 161404.
[7] A.D. Bozhko, et al., "Resistance vs. pressure of single-wall carbon nanotubes," *Applied Physics A: Materials Science & Processing*, vol. 67, 1998, pp. 75-77.
[8] V.T.S. Wong and W.J. Li, "Bundled carbon nanotubes as electronic circuit and sensing elements," *Proc. IEEE International Conference on Robotics and Automation*, 2003, pp. 3648-3653.
[9] T.W. Ebbesen, et al., "Electrical conductivity of individual carbon nanotubes," *Nature*, vol. 382, no. 6586, 1996, pp. 54-56.
[10] Y. Gao and Y. Bando, "Carbon nanothermometer containing gallium," *Nature*, vol. 415, no. 6872, 2002, pp. 599.
[11] Z. Liu, et al., "A novel method for practical temperature measurement with carbon nanotube nanothermometers," *Nanotechnology*, vol. 17, no. 15, 2006, pp. 3681-3684.
[12] P.S. Dorozhkin, et al., "A liquid-Ga-filled carbon nanotube: a miniaturized temperature sensor and electrical switch," *Small*, vol. 1, no. 11, 2005, pp. 1088-1093.
[13] J. Pekola, "Trends in thermometry," *Journal of Low Temperature Physics*, vol. 135, no. 5-6, 2004, pp. 723-744.
[14] J.B. Johnson, "Thermal agitation of electricity in conductors," *Nature*, vol. 119, 1927, pp. 50-51.
[15] J.B. Johnson, "Thermal agitation of electricity in conductors," *Physical Review*, vol. 32, no. 1, 1928, pp. 97-109.
[16] H. Nyquist, "Thermal Agitation of Electric Charge in Conductors," *Physical Review*, vol. 32, no. 1, 1928, pp. 110-113.
[17] F.R. Connor, *Noise*, Edward Arnold, 1982.
[18] W. Schottky, "Regarding spontaneous current fluctuation in different electricity conductors," *Annalen der Physik*, vol. 57, no. 23, 1918, pp. 541-567.
[19] J.R. Pierce, "Physical sources of noise," *Proceedings of the IRE*, vol. 44, no. 5, 1956, pp. 601-608.
[20] L. Spietz, et al., "Primary electronic thermometry using the shot noise of a tunnel junction," *Science*, vol. 300, no. 5627, 2003, pp. 1929-1932.
[21] L. Spietz, et al., "Shot noise thermometry down to 10 mK," *Applied Physics Letters*, vol. 89, no. 18, 2006, pp. 183123.
[22] E. Pop, et al., "Electrical and thermal transport in metallic single-wall carbon nanotubes on insulating substrates," *Journal of Applied Physics*, vol. 101, no. 9, 2007, pp. 093710.
[23] H. Maune, et al., "Thermal resistance of the nanoscale constrictions between carbon nanotubes and solid substrates," *Applied Physics Letters*, vol. 89, no. 1, 2006, pp. 013109.
[24] J.B. Pendry, "Quantum limits to the flow of information and entropy," *Journal of Physics A: Mathematical and General*, vol. 16, 1983, pp. 2161-2171.
[25] K. Schwab, et al., "Measurement of the quantum of thermal conductance," *Nature*, vol. 404, no. 6781, 2000, pp. 974-977.

[26] L. Shi, et al., "Measuring Thermal and Thermoelectric Properties of One-Dimensional Nanostructures Using a Microfabricated Device," *Journal of Heat Transfer*, vol. 125, no. 5, 2003, pp. 881-888.
[27] C. Dames, et al., "A hot-wire probe for thermal measurements of nanowires and nanotubes inside a transmission electron microscope," *Review of Scientific Instruments*, vol. 78, no. 10, 2007, pp. 104903.
[28] A.D. Franklin, et al., "In-place fabrication of nanowire electrode arrays for vertical nanoelectronics on Si substrates," *Journal of Vacuum Science & Technology B: Microelectronics and Nanometer Structures*, vol. 25, no. 2, 2007, pp. 343-347.
[29] M.R. Maschmann, et al., "Vertical single-and double-walled carbon nanotubes grown from modified porous anodic alumina templates," *Nanotechnology*, vol. 17, 2006, pp. 3925-3929
[30] M.R. Maschmann, et al., "Optimization of carbon nanotube synthesis from porous anodic Al-Fe-Al templates," *Carbon*, vol. 45, no. 11, 2007, pp. 2290-2296.
[31] P.J. de Pablo, et al., "Nonlinear Resistance versus Length in Single-Walled Carbon Nanotubes," *Physical Review Letters*, vol. 88, no. 3, 2002, pp. 036804.
[32] P.G. Collins, et al., "1/f noise in carbon nanotubes," *Applied Physics Letters*, vol. 76, no. 7, 2000, pp. 894-896.
[33] S. Reza, et al., "Thermally activated low frequency noise in carbon nanotubes," *Journal of Applied Physics*, vol. 99, no. 11, 2006, pp. 114309.
[34] E.S. Snow, et al., "1/f noise in single-walled carbon nanotube devices," *Applied Physics Letters*, vol. 85, no. 18, 2004, pp. 4172-4174.
[35] J.Y. Huang, et al., "Atomic-Scale Imaging of Wall-by-Wall Breakdown and Concurrent Transport Measurements in Multiwall Carbon Nanotubes," *Physical Review Letters*, vol. 94, no. 23, 2005, pp. 236802-236804.
[36] Y. Wei, et al., "Vacuum-Breakdown-Induced Needle-Shaped Ends of Multiwalled Carbon Nanotube Yarns and Their Field Emission Applications," *Nano Lett.*, vol. 7, no. 12, 2007, pp. 3792-3797.